Available online at www.sciencedirect.com
ScienceDirect
Nuclear Instruments and Methods in Physics Research B 259 (2007) 836–840
NIM B
Beam Interactions with Materials & Atoms
www.elsevier.com/locate/nimb

Stopping power of helium gas for ^{9}Be ions from 2 to 31 MeV

M. Zadro [a,*], A. Di Pietro [b], P. Figuera [b], M. Fisichella [b,c], M. Lattuada [b,c], A. Maggio [b,c], F. Pansini [b,e], M. Papa [d], V. Scuderi [b], O.Yu. Goryunov [f], V.V. Ostashko [f]

[a] *Ruđer Bošković Institute, P.O. Box 180, HR-10002 Zagreb, Croatia*
[b] *INFN Laboratori Nazionali del Sud, Catania, Italy*
[c] *Dipartimento di Fisica ed Astronomia, Catania, Italy*
[d] *INFN Sezione di Catania, Catania, Italy*
[e] *Centro Siciliano di Fisica Nucleare e Struttura della Materia, Catania, Italy*
[f] *Institute for Nuclear Research, Kiev, Ukraine*

Received 17 October 2006; received in revised form 31 January 2007
Available online 21 February 2007

Abstract

The stopping power of helium gas for ^{9}Be ions from 2 to 31 MeV is experimentally determined using an indirect method. The residual energy of the ^{9}Be beam as a function of the gas thickness is measured and the stopping power determined by differentiating the thickness–energy curve. The results are compared with predictions of the semi-empirical codes SRIM-2003 and MSTAR. Our data are in better agreement with the MSTAR calculations. The elastic scattering excitation function for the system ^{9}Be + α, extracted using the thick target technique and our stopping power data, is in excellent agreement with the ones measured directly confirming the quality of our data.

PACS: 34.50.Bw; 25.40.Ny

Keywords: Stopping power; ^{9}Be ions; Helium gas; Resonance scattering

1. Introduction

The use of thick gas targets and inverse kinematics is a very efficient method for the study of resonance scattering of low intensity radioactive beams and light nuclei [1]. In these experiments a scattering chamber is filled with gas that acts at the same time as target and as beam degrader. The method allows the measurement of the scattering excitation function in a wide energy region with one single beam energy. The excitation function is reconstructed from the measured energy spectra of the recoiling light particles by taking into consideration the two-body kinematics and energy losses of the projectile before the interaction and of the recoil after the interaction. Thus, the stopping power data are essential for a correct extraction of the excitation function measured with this technique.

A set of resonance scattering experiments on *infinite* ^{4}He targets are planned at the forthcoming radioactive ion beam (RIB) facility EXCYT at Laboratori Nazionali del Sud (LNS) in Catania. The EXotics with CYclotron and Tandem (EXCYT) facility uses two-accelerator isotope separation on-line (ISOL) technique for production of radioactive beams (see e.g. [2]). A preliminary experiment was performed with stable beams in order to test the experimental set up [3]. One of the systems studied was ^{9}Be + α. The ^{9}Be beam was chosen because its mass is close to the ones of the exotic beams of interest (^{8}Li and ^{9}Li). In fact, it is well known that the resolution obtained with this kind of experiments depends on the projectile-target mass ratio, see e.g. [4]. Moreover, the elastic excitation function of the ^{9}Be + α system has been measured [5,6] with standard thin target experiments by varying the ^{4}He beam energy. The

* Corresponding author. Tel.: +385 1 4561 109; fax: +385 1 4680 239.
E-mail address: zadro@irb.hr (M. Zadro).

0168-583X/$ - see front matter © 2007 Elsevier B.V. All rights reserved.
doi:10.1016/j.nimb.2007.02.078

strong resonance observed at $E_{c.m.} \approx 3.5$ MeV in these experiments [5,6] can represent a good reference for comparison.

The elastic scattering measurement was performed at LNS using the CT2000 scattering chamber having a diameter of 2 m which was filled with helium gas at a pressure of 428.3 mbar. A schematic drawing of the experimental setup is shown in Fig. 1. The ^{9}Be beam was delivered by the SMP Tandem Van de Graaf accelerator of the LNS. The beam energy after a Kapton entrance window was 29.95 MeV. The gas pressure and temperature were monitored by the same system used for the stopping power measurement described in the next section. Two large $\Delta E - E$ silicon telescopes (65 μm + 500 μm thick) were placed in the forward part of the chamber to detect and identify α-particles recoiling in a finite angular range around 180° in the center of mass (c.m.) system. A microchannel plate (MCP) detector was mounted just before the entrance window to measure the beam intensity, which was of the order of 10^5 pps, and to produce a fast signal for time of flight measurement. The time difference between the MCP and ΔE detector signals was successfully used to separate the elastic scattering events from inelastic scattering contributions [3].

The SRIM-2003 tables [7] for the stopping powers of helium for ^{9}Be and ^{4}He impinging ions were used in the analysis of the ^{9}Be + α scattering. Fig. 2 shows the low energy part of the scattering excitation function deduced from our experiment for the detector placed at about 0°, corresponding to α-particles stopped in the ΔE detector. Due to the used technique (see e.g. [8]), different c.m. energies correspond to different c.m. scattering angles (shown in the upper scale of Fig. 2). For comparison we also show

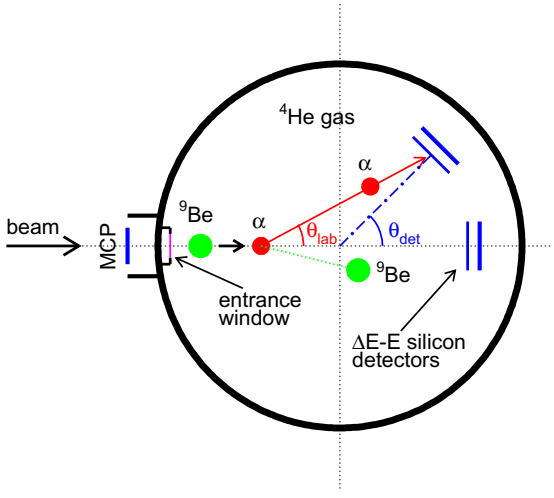

Fig. 1. A schematic drawing of the experimental setup used for measuring the elastic scattering excitation function. θ_{lab} is the recoil angle of the α-particle and θ_{det} is the corresponding detection angle relative to the center of the scattering chamber. Note that for a given θ_{det} the angle θ_{lab} depends on the position of the interaction between the ^{9}Be projectile and the α-particle. The scattering angle in the center of mass (c.m.) system is given by $\theta_{c.m.} = 180° - 2\theta_{lab}$ (see [4]).

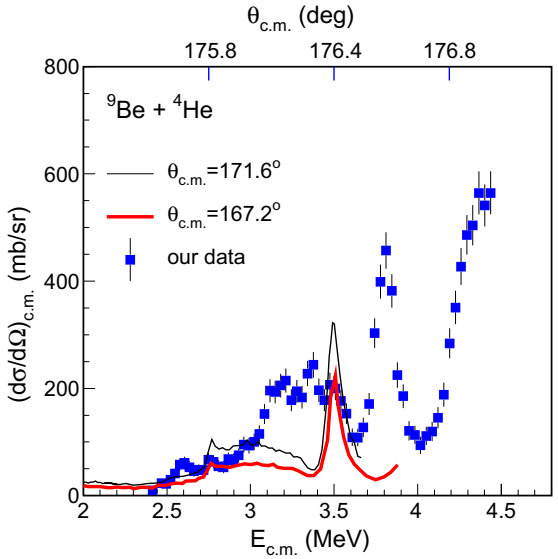

Fig. 2. ^{9}Be + α elastic scattering excitation function deduced from our experiment for the detector at 0°. Stopping powers for ^{9}Be and ^{4}He in helium were taken from SRIM-2003. The thick and thin lines show the data of [5] and [6], respectively, obtained using ^{4}He beams impinging onto thin ^{9}Be targets. The upper scale shows the mean c.m. scattering angles for our experiment (see text for details).

the excitation functions for the same system measured by Goss et al. [5] (thick line) and Liu et al. [6] (thin line) in standard experiments using thin ^{9}Be targets and varying the ^{4}He beam energy. As seen in Fig. 2, there are large differences between our excitation function and those of [5] and [6]. These differences can be attributed to the inaccurate stopping powers used to transform the experimental α-particle spectrum into the excitation function.

An experiment was therefore performed in order to measure the stopping power of helium for ^{9}Be ions in the energy range of our interest ($E \lesssim 30$ MeV). To our knowledge, no stopping power measurements for this ion-target combination have been reported so far.

2. Experimental procedure

The ^{9}Be + α stopping power measurement was performed in the same reaction chamber used for the resonance scattering experiment. A 13 μm thick Kapton window was used to separate the chamber from the beam line. The chamber was filled with helium gas and the energy of ^{9}Be beam inside the chamber was measured at different distances from the Kapton window and for several values of the gas pressure.

Three silicon surface barrier detectors were mounted in the chamber on a movable support so that each of them in turn could be placed along the beam direction (i.e. at 0°). The energy of the ^{9}Be beam was measured directly in the detector keeping the beam intensity lower than 10^3 pps. The ^{9}Be path lengths in the gas, corresponding to the three detectors, were 109.8, 139.6 and 180.6 cm and were measured with an estimated accuracy of ±2 mm.

Commercially available helium gas, with nominal purity of 99.9999%, was used in the experiment. The helium pressure was controlled with a capacitance manometer (MKS Instruments 122AAX). The calibration of the manometer was performed by MKS just before the experiment, giving a precision in the measured values of the order of 0.3% in the range of interest. The temperature was measured within ±1 K with a thermocouple set inside the chamber. The path length, pressure and temperature were converted into gas thickness (expressed in mg/cm^2) using simple pressure and temperature scaling and $\rho_0 = 1.66322 \times 10^{-4}$ g/cm^3 for helium density at $P = 1013.25$ mbar, $T = 20$ °C [9].

A standard α-source containing ^{239}Pu, ^{241}Am and ^{244}Cm was used for detector calibration. In addition, a ^{9}Be beam at 22.97 and 34.17 MeV was used to provide calibration points in the range of higher energies. The ^{9}Be beam energies were determined from the resonance frequency of the nuclear magnetic resonance Gaussmeter of the 90° analysing magnet after the tandem accelerator. Energy losses of the α-particles and ^{9}Be ions in the detector entrance window (40 μg/cm^2 of gold) were taken into account. The corrected energies as a function of the observed pulse height were well fitted by a straight line using the least squares method. The electronic offset was determined using a precision pulse generator (BNC-PB4) and was used in the calibration fit as the zero-energy point. Moreover, in order to have a continuous control of the stability of the electronics, signals from the pulser were sent to the test input of the preamplifiers and recorded during the whole measurement.

The measurements were performed using a ^{9}Be energy of 31.56 MeV after the Kapton window. Residual energy spectra were measured at 26 different pressures between 50.6 and 420.8 mbar. The mean value of the residual energy, E, for a given gas thickness, d, was determined from the measured energy distribution by taking into account the channels containing more than ~10% of the maximum intensity [10,11]. The thickness versus energy curve with about fifty points was then constructed from the data.

3. Analysis and results

The mean incident energy E_0, the target thickness d and the mean energy E of the ions after traversing the thickness d are related by the following formula:

$$d = \int_E^{E_0} \frac{1}{S(E')} \mathrm{d}E', \tag{1}$$

where $S(E)$ is the stopping power. The experimental thickness–energy curve was fitted with a polynomial of the form

$$d = \sum_{i=0}^{n} a_i E^i, \tag{2}$$

by using the least squares method. Then the stopping power $S(E)$ was calculated from the fitting parameters a_i by differentiating this curve,

$$\frac{\mathrm{d}d}{\mathrm{d}E} = -\frac{1}{S(E)} = \sum_{i=1}^{n} i a_i E^{i-1}, \tag{3}$$

Similar indirect procedures have been used by a number of authors, see e.g. [10,11].

The thickness–energy data are shown in Fig. 3. The data obtained with the three different detectors are represented by different symbols. The good agreement between the three data groups confirms the consistency of the experiment.

The whole data set was fitted by a single polynomial. The reduced chi-squares χ^2 for several polynomial degrees n were compared to estimate the most adequate value of n. It was found that χ^2 does not change significantly for $n \geqslant 7$. The results of the fit for $n = 7$ are shown by the solid line in Fig. 3. The results for the stopping power are shown in Fig. 4 and in Table 1 for integer values of energy. The fitting parameters a_i, $i = 1$–7, are given in Table 2. The results of the fit with $n = 8$ do not differ considerably from those for $n = 7$. The largest differences between the stopping power values obtained with $n = 7$ and $n = 8$ are between +1.3% and −0.5% in the energy range $2 < E < 5$ MeV and the results agree to within ±0.3% for $E > 5$ MeV.

Corrections were made to take into account the effects of deformation of the Kapton window due to the gas pressure. The deformation of the window results in an increase Δl in the path length l and a decrease Δt in the window thickness t. These deformations were calculated using the model of Hencky, see [12]. The measured path lengths were then increased by Δl to take into account the window bending. The decrease Δt in the window thickness leads to an increase ΔE_0 in the incident ion energy E_0 such that $\Delta E_0/\Delta E_w \approx \Delta t/t$, where ΔE_w is the energy loss in the window which was measured with empty chamber. Since the present method of analysis assumes a constant incident energy,

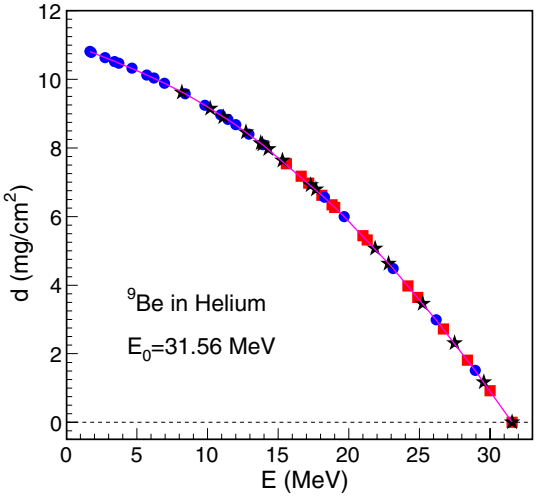

Fig. 3. Thickness–energy curve for ^{9}Be ions in helium gas for an initial ^{9}Be ion energy of 31.56 MeV. The different symbols correspond to the experimental data obtained with the three different detectors. The data are corrected for the effects of window deformation (see text). The solid line is the result of the fit with a 7th degree polynomial.

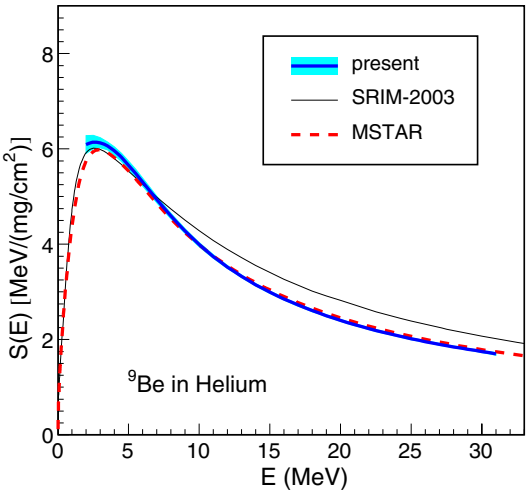

Fig. 4. Measured stopping power values for ^{9}Be ions in helium gas compared to values calculated with SRIM-2003 and MSTAR. The shaded area represents the estimated errors of the measured values.

Table 1
Present experimental stopping power data for ^{9}Be in helium gas. E is given in MeV and $S(E)$ in MeV/(mg/cm^2)

E	$S(E)$	E	$S(E)$	E	$S(E)$
2.0	6.09 ± 0.18	12.0	3.522 ± 0.030	22.0	2.230 ± 0.021
3.0	6.13 ± 0.11	13.0	3.325 ± 0.026	23.0	2.154 ± 0.021
4.0	5.958 ± 0.085	14.0	3.151 ± 0.026	24.0	2.083 ± 0.020
5.0	5.660 ± 0.089	15.0	2.994 ± 0.026	25.0	2.017 ± 0.019
6.0	5.304 ± 0.081	16.0	2.853 ± 0.025	26.0	1.957 ± 0.018
7.0	4.940 ± 0.068	17.0	2.725 ± 0.024	27.0	1.900 ± 0.018
8.0	4.593 ± 0.057	18.0	2.609 ± 0.023	28.0	1.848 ± 0.018
9.0	4.277 ± 0.050	19.0	2.502 ± 0.022	29.0	1.797 ± 0.018
10.0	3.994 ± 0.043	20.0	2.404 ± 0.021	30.0	1.749 ± 0.019
11.0	3.743 ± 0.036	21.0	2.313 ± 0.021	31.0	1.701 ± 0.027

the gas thicknesses calculated from the corrected path lengths were decreased by Δd, the thickness of helium which reduces the incident beam energy by ΔE_0, $\Delta d = \int_{E_0}^{E_0+\Delta E_0} dE/S(E) \approx \Delta E_0/S(E_0)$. The stopping power $S(E_0)$ used for the calculation of Δd was obtained from the fit to non-corrected data. The effects of these corrections on the stopping power values were small, typically less then 0.3%, except in the upper part of our energy range ($E \gtrsim 25$ MeV) where they were up to ~1%.

The errors in the measured stopping power data result from the random and systematic errors of the measurement. The random measurement errors were estimated from the reduced χ^2 by assuming a good fit, as discussed in [13]. The contribution of these errors to the uncertainty in the stopping power was then calculated from the covariance matrix of the fitted parameters. The main contributions to the systematic error come from the uncertainty of the gas temperature (±1 K), the pressure measurement (±0.3%) and the uncertainty of the path length determination (±2 mm). The total estimated errors in the stopping power data are ~±3% at $E = 2$ MeV, decreasing to ±1.6% at $E = 5$ MeV and to ~±1% at $10 < E < 30$ MeV. The stopping power values obtained from the fit with $n = 8$ are within these errors.

The effects of the pulse height defect (PHD) of detectors [14] were also considered. The main contributions to the PHD come from the energy loss in the detector dead layer (the window defect) and the energy loss in non-ionizing processes in the active layer (the nuclear defect), see e.g. [15]. These effects lead to a non-linear and ion-dependent detector response. The window defect was taken into account in our calibration. We repeated the analysis including the effects of the nuclear defect. The ionization energy loss of α-particles and ^{9}Be ions in silicon was calculated by the SRIM Monte Carlo code [7]. The effect of the PHD correction on the results for the stopping power was small, much smaller than the estimated errors in the stopping power values.

The thin solid and thick dashed lines in Fig. 4 represent the calculated stopping power values from the semi-empirical codes SRIM-2003 [7] and MSTAR [16], respectively. Compared to the results of both calculations, our results

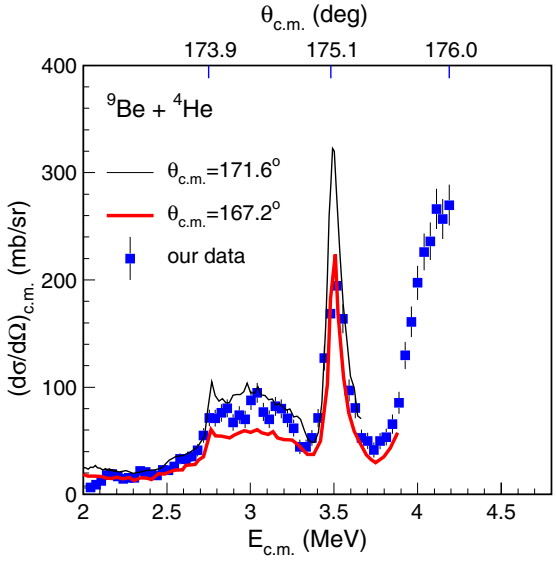

Fig. 5. ^{9}Be + α scattering excitation function deduced from our experiment for the detector at 0°. Experimental data were used for the stopping power of helium for ^{9}Be whereas the stopping power of helium for the recoiling α-particles was calculated using ASTAR [17]. The thick and thin lines show the data of [5] and [6], respectively, obtained using direct kinematics and thin targets. The upper scale shows the mean c.m. scattering angles for our experiment.

Table 2
Parameters for calculation of $S(E)$, in MeV/(mg/cm^2), of helium gas for ^{9}Be ions over the energy region $E = 2 - 31$ MeV (Eq. (3))

$a_1 = -1.9061 \times 10^{-1}$	$a_2 = 1.1852 \times 10^{-2}$	$a_3 = -2.0358 \times 10^{-3}$	$a_4 = 1.1863 \times 10^{-4}$
$a_5 = -4.0135 \times 10^{-6}$	$a_6 = 7.3312 \times 10^{-8}$	$a_7 = -5.5691 \times 10^{-10}$	

(thick solid line) are higher in the region of the stopping power maximum; differences are within 3% for $3 < E < 6$. One sees significant differences between the present results and the SRIM-2003 calculations at higher energies. Above ~7 MeV the present values are lower than the SRIM-2003 calculations; differences are ~15.5% at $E > 20$ MeV. On the other hand our data are in agreement with the MSTAR code to within ±2.6% above 3 MeV.

We have reanalysed our data for the ^{9}Be+^{4}He scattering excitation function using the experimental values of the stopping power for ^{9}Be in helium. The stopping power for ^{4}He in helium was calculated by the program ASTAR [17]. The results are shown in Fig. 5. As can be seen, our new excitation function is in good agreement with the existing data [5,6]. The use of the SRIM-2003 values of the stopping power for ^{4}He in helium results in a slight shift of the excitation function, of the order of 20 keV. The SRIM-2003 and ASTAR stopping powers for ^{4}He in helium agree to <3% for the ^{4}He energies of our interest (~0.5–30 MeV).

4. Summary and conclusions

The stopping power values of helium gas for ^{9}Be ions with energies between 2 and 31 MeV have been measured. The experimental method employed consists in measuring the energy of incident ions after traversing different target areal densities. A polynomial expression was fitted to the measured thickness–energy curve and the stopping power was obtained by analytical differentiation. The estimated uncertainties of the stopping power values are typically less than ±2%.

The results of the measurement were compared with the predictions of the semi-empirical stopping power codes SRIM-2003 and MSTAR, showing a better agreement with the MSTAR values which is within ±2.6% for $3 < E < 31$ MeV.

The experimental stopping power was used in the analysis of the $^{9}\mathrm{Be} + {}^{4}\mathrm{He}$ scattering data measured using the method of inverse kinematics and thick gas target. The good agreement between the scattering excitation function deduced from our measurement and those obtained with conventional experiments confirms the reliability of our stopping power data.

Acknowledgement

O.G., V.O. and M.Z. would like to thank the LNS for the warm hospitality as well as for the financial support.

References

[1] V.Y. Goldberg et al., Phys. Rev. C 69 (2004) 024602 (and references therein).
[2] G. Ciavola et al., Nucl. Phys. A 701 (2002) 54c.
[3] A. Di Pietro et al., LNS Activity Report (2004) 242;
V. Scuderi et al., Eur. Phys. J. A, submitted for publication.
[4] K. Markenroth et al., Phys. Rev. C 62 (2000) 034308.
[5] J.D. Goss, S.L. Blatt, D.R. Parsignault, C.D. Porterfield, F.L. Rifle, Phys. Rev. C 7 (1973) 1837.
[6] J. Liu, Z. Zheng, W.K. Chu, Nucl. Instr. and Meth. B 108 (1996) 247.
[7] J.F. Ziegler, Nucl. Instr. and Meth. B 219–220 (2004) 1027;
J.F. Ziegler, SRIM-2003 version 26. <http://www.srim.org>.
[8] G.V. Rogachev, Ph.D. thesis, Russian Research Centre Kurchatov Institute, 1999 (in Russian).
[9] Material composition data used by ASTAR [17]. <http://physics.nist.gov/cgi-bin/Star/compos.pl?ap>.
[10] C. Hanke, J. Laursen, Nucl. Instr. and Meth. 151 (1978) 253.
[11] D.I. Thwaites, Phys. Med. Biol. 25 (1980) 865.
[12] W.B. Fichter, NASA Technical Paper 3658, NASA Langley Research Center, 1997.
[13] W.H. Press, S.A. Teukolsky, W.T. Vetterling, B.P. Flannery, Numerical Recipes in Fortran 77: The Art of Scientific Computing, second ed., Cambridge University Press, Cambridge, 1992.
[14] G.F. Knoll, Radiation Detection and Measurement, Wiley, New York, 1979.
[15] L. Cliche, S.C. Gujrathi, L.A. Hamel, Nucl. Instr. and Meth. B 45 (1990) 270.
[16] H. Paul, A. Schinner, Nucl. Instr. and Meth. B 195 (2002) 166;
H. Paul, MSTAR version 3.21. <http://www.exphys.uni-linz.ac.at/stopping/>.
[17] M.J. Berger, J.S. Coursey, M.A. Zucker, and J. Chang (2005), ESTAR, PSTAR, and ASTAR: Computer Programs for Calculating Stopping-Power and Range Tables for Electrons, Protons, and Helium Ions (version 1.2). <http://physics.nist.gov/PhysRefData/Star/Text/contents.html>, National Institute of Standards and Technology, Gaithersburg, MD, USA.